Nonhomogeneous textures and banded flow in a soft cubic phase under shear

E. Eiser,* F. Molino, and G. Porte*
Groupe de Dynamique des Phases Condensées,† Université Montpellier II, F-34095 Montpellier Cedex 05, France

O. Diat
European Synchrotron Radiation Facility, Boîte Postale 220, F-38043 Grenoble Cedex, France
(Received 30 August 1999)

We report evidence for two distinct strain-induced orientation transitions in a lyotropic bcc cubic crystal submitted to increasing shear rates. The crystal is built up from copolymer spherical micelles in a selective solvent. The distribution of orientations is characterized by x-ray diffraction: in the two oriented states, the dense ⟨111⟩ rows align along the flow, but they differ from each other in the orientations of the dense layers with respect to the shear plane. These orientation transitions have clear rheological signatures in the form of two stress plateaus each associated with the coexistence of two states of orientation. We compare this behavior with the well documented shear-induced orientation transition in wormlike micelles.

PACS number(s): 82.70.Dd

INTRODUCTION

Since the pioneering studies of Clark and Ackerson [1–3] in the early 1980s, it has been known that, when colloidal crystals are sheared, they often undergo a structural transition such that dense layers are arranged to minimize the resistance against flow: the close packed direction aligns parallel to the flow direction and the planes of highest density stack parallel to the shear plane. The regime for which the applied shear rate induces such an alignement of the dense planes is referred to as the layer-sliding regime, as the layers can glide past each other and thus accommodate the shear stress. On the other hand, the mechanical response associated with such shear-induced alignment is to date much less well documented [4,5]. In one case [5], nevertheless, scattering data collected together with rheological measurements revealed that a nonmonotonic evolution of the stress response to increasing rates could be unambiguously assigned to an orientation transition. But colloidal crystals often have large lattice spacings (on the micrometer scale) and as a consequence the shear moduli and the yield stress are very low and difficult to measure in conventional rheometry. More recently, block copolymers either in melts or in selective solvents were reported to self-assemble into spherical micelles which under appropriate conditions pack into similar crystalline structures [6–8]. Depending on the relative sizes of the dense core and the swollen corona of the micelles, ruling the interparticle interactions, either fcc or bcc crystals are obtained with lattice spacings of the order of 10 nm. Their mechanical stiffness is more suitable for rheometry. Orientation under shear has been observed by neutron or x-ray diffraction several times [9–12].

In a different context, banded inhomogeneous flows have been reported frequently in wormlike micelle solutions [13–17] under shear with a characteristic shear rate $\dot{\gamma}_t$. The mechanical signature is the onset of a stress plateau at $\dot{\gamma}_t$ where the stress abruptly becomes independent of the shear rate. Optical birefringence as well as neutron scattering revealed the following. Below $\dot{\gamma}_t$ the wormlike micelles behave like entangled polymer coils in a semidilute solution. Above $\dot{\gamma}_t$, and thus in the plateau region, a birefringent band of strongly oriented micelles appears in coexistence with the nonoriented entangled low-shear structure. The portion of the new shear-aligned structure increases with the shear rate until the entire volume is filled up by the new structure: this behavior is analogous to that of a ''first order'' orientation transition. Stress plateaus associated with banded flows have also been reported for other self-assembling systems having completely different microstructures: smectic swollen lamellar phases [18] and giant highly deformable vesicles [19] in surfactant systems. Hence this flow mechanism seems very general.

In the present article, we investigate the structure and mechanical response of a micellar cubic phase (bcc) in an aqueous triblock copolymer solution submitted to shear. We observe not only one but two separate orientation transitions upon increasing shear rates. The first is from a disoriented polycrystalline texture to a fully oriented twinned bcc crystal with the line of highest particle density along the ⟨111⟩ direction parallel to the velocity and the {211} planes parallel to the shear plane. At still higher shear rates a second transition occurs to another fully oriented pattern again with the dense direction ⟨111⟩ parallel to the velocity and the {110} planes parallel to the shear plane. These orientation patterns are evidenced from x-ray scattering under shear using a specially designed Couette cell. X rays further show that, at the rates where distinct patterns coexist, they are organized in space into bands parallel to the shear plane. As in wormlike micelle solutions strong shear thinning occurs. However, we observe not only one but two stress plateaus in the flow curve. They correspond to two coexistences of differently oriented dense planes. This implies that both transitions are shear thinning, the high-shear state being more fluid than the low-shear one.

*Authors to whom correspondence should be addressed. Electronic addresses: porte@gdpc.univ-montp2.fr, eiser@gdpc.univ-montp2.fr

†GDPC is ''unité mixte de recherche CNRS/UMII No. 5581.''

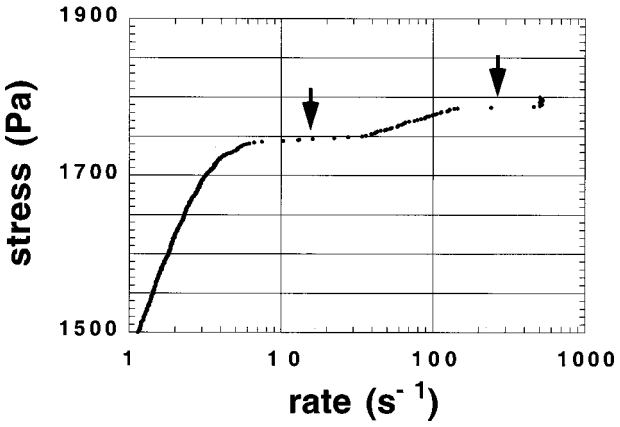

FIG. 1. Shear stress versus shear rate for the 46% sample at 20 °C.

EXPERIMENTS AND RESULTS

The cubic phase is obtained from a triblock copolymer commercially available from SERVA under the name Synperonic F68: $(EO)_{76}$-$(PO)_{29}$-$(EO)_{76}$, where EO is ethylene oxide, and PO is propylene oxide. With no further purification we produce solutions in pure water at suitable concentrations (all data shown are taken from 46 wt. % probes). Water acts as a selective solvent: at low temperatures, typically 5 °C, all chains are solvated. As the temperature is increased, however, water becomes a less good solvent for the PO middle block and the copolymer self-assembles into spherical micelles with a dense, water-free PO core and a hydrated EO corona. At polymeric concentrations above 40 wt. %, a liquid to solid transition is observed when coming from low to room temperature. Small angle x-ray diffraction reveals that this solid phase is of polycrystalline body-centered cubic structure. Crystallization upon heating eases the sample preparation, so the shear cell is filled up with solution at low temperature and brought to the desired temperature afterward. Thus we get crystallized samples that have not been submitted to any irreversible plastic deformation before measurement.

The rheological behavior is measured using a stress controlled rheometer (Physica UDS 200) in the cone-plate geometry (the plate diameter is 50 mm with an inclination angle of 1°). The flow curve in Fig. 1 is obtained by applying a relatively low stress to the unsheared polycrystalline sample. The stress was then increased in steps of 1 Pa. The strain rate was measured after 4 s, which proved to be sufficient to reach the steady state. The flow curve clearly shows two distinct ranges in shear rate over which the stress almost completely levels off and saturates. The first plateau spans the rate range from 6 to 40 s^{-1} and the second one from 130 to 400 s^{-1}. It is interesting to note that the two plateaus are extremely close to one another in terms of the value of the total stress: at 1740 and 1785 Pa, respectively, and thus with a relative stress separation of only 2.5%. Within each of these plateaus, we expect two distinct structural organizations of the sheared material to coexist in the gap, each one having a different effective viscosity. The presence of two plateaus implies that three different textures should appear successively at increasing stresses. To investigate this aspect, we switch to x-ray diffraction under shear.

All diffraction data are obtained at line ID2 at the European Synchroton Radiation Facility using a Couette cell transparent to x rays, rotated at controlled speed by a dc-current electric motor. No device is used to measure the torque, so the average shear rate is monitored but not the stress. The radius of the cell is 10 mm and the width of the gap is 1 mm. Due to this width to radius ratio, the stress is not constant through the gap but increases monotonically by 20% from the outer toward the inner wall. As a consequence, the strain rate is not homogeneous either: therefore all shear rates reported hereafter for the scattering cell are average shear rates calculated from the velocity of the rotating inner bob. The radial geometry (with the x-ray beam parallel to the velocity gradient) and the tangential geometry (x-ray beam impinging the Couette gap tangentially, and thus parallel to the velocity) were used. Moreover, the narrow width of the beam ($\sim$150 μm) allows one to explore the 1 mm gap slice by slice in the tangential geometry. The x-ray wavelength was 1 Å with a resolution $\Delta\lambda/\lambda = 0.01$, and a sample to detector distance of 4 m.

At high shear rates, we could not prevent interfacial instabilities which quickly ruined the homogeneity of the samples (proliferating bubbles). To avoid this difficulty, we first checked carefully that with shearing at any rate the steady state of orientation was reached after a short time only (ten to twenty strain units at most). Scattering patterns taken while shearing at any given steady rate and after abrupt cessation of shear are identical. This allowed us to measure all spectra at rest right after having presheared the sample at the rate of interest for a short time only: the scattering patterns so obtained are entirely determined by the latest preshear rate and insensitive to the previous shear history of the sample [20].

After crystallization *in situ*, a sample that has never been sheared shows spherically averaged powder diffraction signatures (not shown here) corresponding to a bcc lattice with a unit cell of 74 Å. After shearing at low rates (1.6 s^{-1} in Fig. 2), below the first stress plateau, the diffraction patterns still indicate a polycrystalline texture but with a weak preferred orientation: the scattered intensity along the Bragg ring is not completely isotropic but reinforced along banana-like patterns corresponding to the orientation distribution of the microcrystals. At the other extreme situation, after very high preshear rates [365 s^{-1} in Fig. 3(a)], the scattering in the radial geometry consists of sharp dots revealing very strong orientation, belonging to the ordered bcc crystal with 74 Å lattice size [indicated by the ''1'' in Fig. 3(a)] and its twin structure (Bragg spots labeled with 1′). The pattern seen in the tangential geometry [Fig. 3(b)] also shows strong orientation around the $\vec{\nabla}$ axis, which is here perpendicular to the diffraction pattern in the q_y-q_z plane. These two patterns reveal a homogeneous orientation of the bcc lattice with the dense $\langle 111 \rangle$ direction parallel to $\vec{\nabla}$ and the dense $\{110\}$ planes parallel to the shear plane (q_x-q_z): this is the well known layer-sliding regime first reported by Ackerson and Clark [3].

The scattering patterns obtained in the radial geometry after preshear at rates in between the above extreme cases are shown in Figs. 4(a)–4(c). At 16 s^{-1}, right in the first stress plateau [Fig. 4(a)], two ellipsoidal reinforcements appear, located vertically on the first order ring, superimposed on the weakly oriented diffuse distribution characteristic of lower

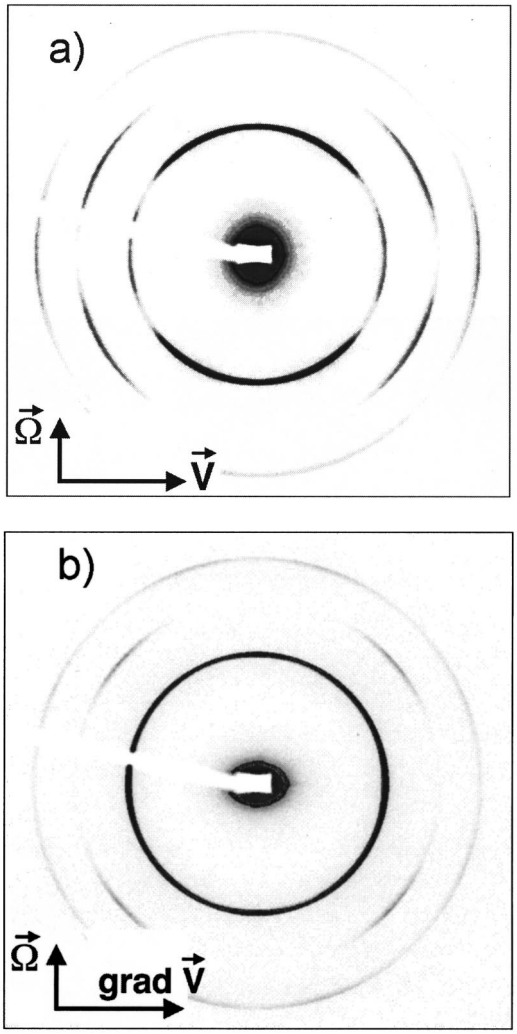

FIG. 2. Scattering pattern after preshearing at 1.6 s^{-1}. (a) Radial geometry: $\vec{V}$ is horizontal and $\vec{\Omega}$ is vertical; (b) tangential geometry: $\nabla\vec{V}$ is horizontal and $\vec{\Omega}$ is vertical.

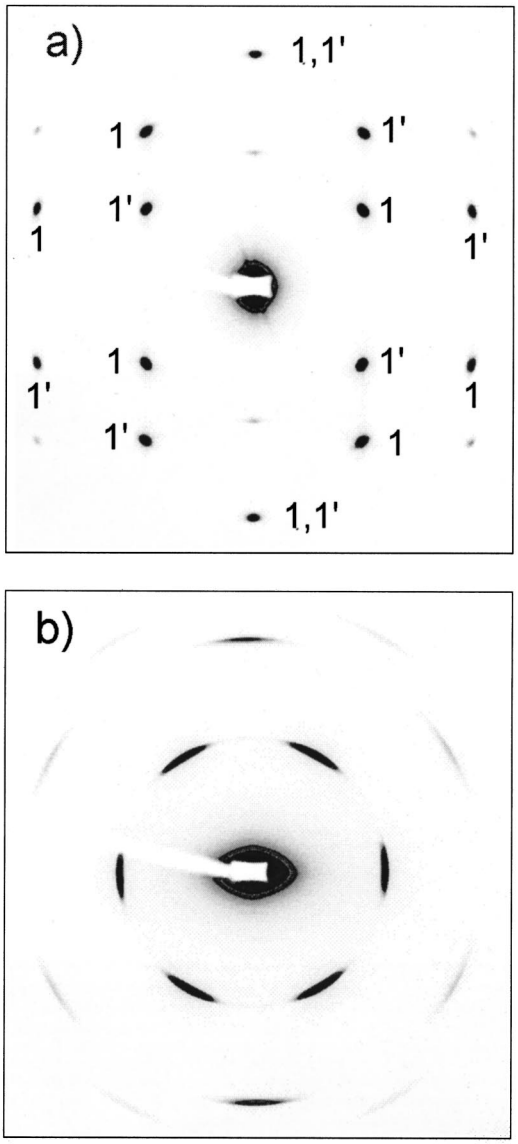

FIG. 3. Scattering pattern after preshear at 365 s^{-1}. (a) Radial geometry (the Bragg spots denoted 1 and 1′ correspond to twin configurations of a similarly oriented bcc lattice completely symmetrical with respect to the velocity direction [3]); (b) tangential geometry.

rates [compare Fig. 2(a)]: we clearly have two coexisting states of orientation in the gap. At 50 s^{-1} [Fig. 4(b)], we still observe the diffuse rings but they are very faint. The upper and lower ellipsoidal reinforcements are very strong and, in addition, we see the set of sharp dots characteristic of layer sliding [as in Fig. 3(a)]. So, at 50 s^{-1}, we have the coexistence of three distinct states of orientation. At higher rates [160 s^{-1} in Fig. 4(b)], within the second plateau, the diffuse rings have completely disappeared but the upper and lower ellipsoidal dots as well as the ''layer-sliding'' set of sharp dots coexist simultaneously with roughly identical proportions. Only at very high rates [Fig. 2(a)] do we get a pattern almost completely dominated by the layer-sliding orientation alone. So, as expected from the rheological data, scattering data also reveal three distinct states of orientation. The pure low-shear weakly oriented state and the pure layer-sliding state are, respectively, obtained at the lowest and highest rates. In principle, we should observe the pure intermediate state (corresponding to the upper and lower ellipsoidal reinforcements) at the appropriate shear rates (40–130 s^{-1}; see Fig. 1). However, as mentioned above, the stress in the Couette cell increased by 20% when moving from the outer to the inner wall. This is much larger than the 2.5% separating the two stress plateaus. Thus, the intermediate orientation state can only appear in combination with the disoriented state (16 s^{-1}) or with the layer-sliding state (160 s^{-1}) or with both of them (50 s^{-1}).

Since the beam is very thin (150 μm diameter), we can resolve the states of orientation at different depths within the gap thickness in tangential geometry, by simply moving the cell laterally relative to the beam in steps of 0.1 mm. To characterize the intermediate state of orientation, we show in Fig. 5 the scattering obtained after 160 s^{-1} in tangential geometry close to the outer wall of the Couette cell: at this rate, the intermediate state coexists with the layer-sliding state [Fig. 4(c)]. But we expect it to be located in the region of the gap where the stress is lower; that is, close to the outer wall. The hexagonal distribution of the intensity along the Bragg rings, together with the upper and lower dots on the first

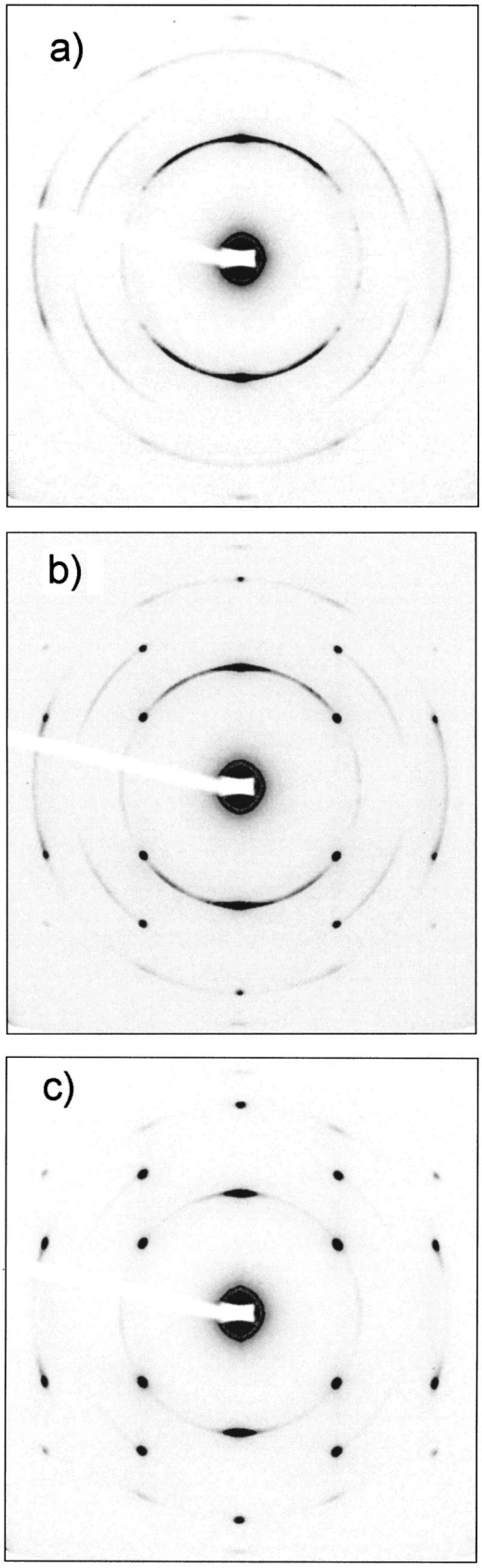

FIG. 4. Scattering pattern in the radial geometry: (a) after 16 s^{-1}, (b) after 50 s^{-1}, and (c) after 160 s^{-1}.

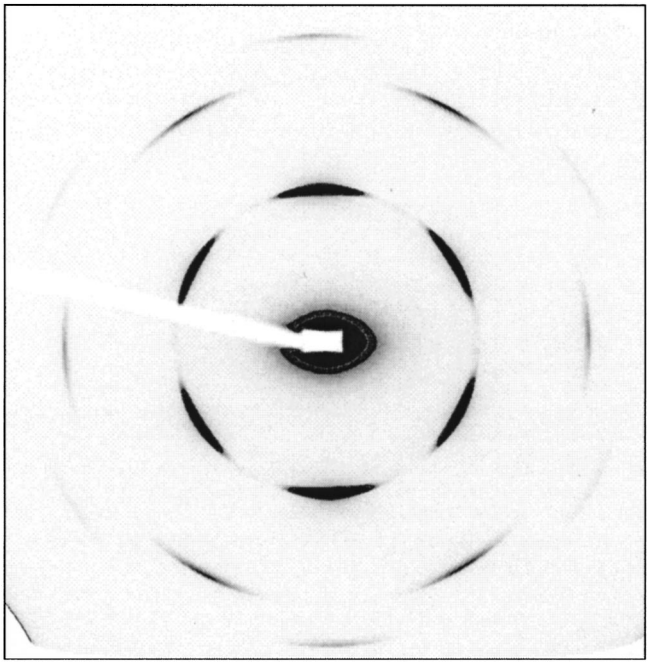

FIG. 5. Scattering pattern in the tangential geometry close to the outer wall of the Couette cell after preshearing for 160 s^{-1}.

ring in the radial geometry, correspond to an orientation different from that of the layer-sliding state [compare with Fig. 3(b)]: the dense $\langle 111 \rangle$ direction still remains along the velocity $\vec{V}(q_x)$ but the dense planes $\{110\}$ are perpendicular to the shear plane with their normal parallel to the vorticity $\vec{\Omega}(q_z)$. In this orientation, the planes that align parallel to the shear plane are the $\{211\}$ planes [see Figs. 6(c) and 6(d) and compare to Figs. 6(a) and 6(b)]. Furthermore, in the tangential geometry, close to the inner wall where the stress is higher, we indeed observe a scattering signature similar to that in Fig. 3(b) indicating that this part of the gap is in the layer-sliding regime. Similarly, we scanned the gap in the tangential geometry after preshearing at 50 s^{-1}; the three distinct states organized in bands as schematized in Fig. 7 were observed one after the other when moving from the outer to the inner wall, as suggested by the superimposed patterns seen in the radial geometry [Fig. 4(b)].

DISCUSSION

Our investigation combining x-ray diffraction under shear and rheometry reveals an unexpectedly rich sequence of orientation patterns: not only do we find one orientation transition upon increasing rates but two successive transitions occurring at very different rates but separated by a very narrow difference in stresses. At low rates, a viscous polycrystalline state fills up the gap; at intermediate rates, a first oriented state is seen with the $\{211\}$ planes parallel to the shear plane; at high rates, we find a second oriented state with the $\{110\}$ planes parallel to the shear plane. In both oriented states, the dense direction, $\langle 111 \rangle$, is along the velocity. Such orientations were previously reported in asymmetric copolymer melts by Koppi *et al.* [10] and in selective solvents by Hamley *et al.* [21]. Here we show that these orientations correspond to separate steady states. Provided the preshear is applied at the rate of interest for sufficient time (a few strain

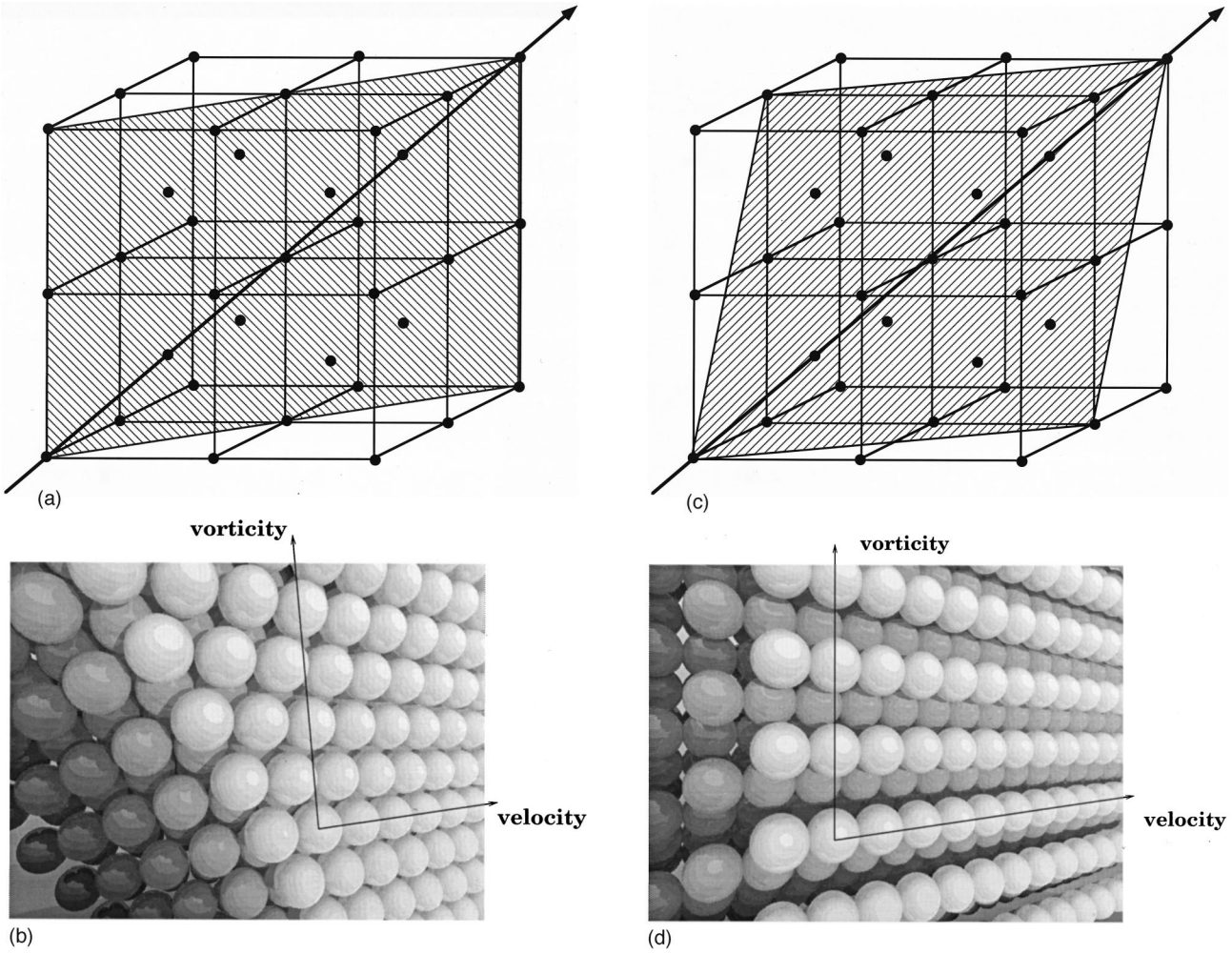

FIG. 6. (a) bcc lattice with a {110} dense plane shaded. (b) Section of a bcc lattice along a {110} dense plane: high shear rate orientation (300 s^{-1}). (c) bcc lattice with a {211} plane shaded. (d) Section of a bcc lattice along a {211} plane: intermediate shear rate orientation.

units are in fact sufficient), a reproducible state of orientation is seen, independent of the former shear history of the sample (e.g., the polycrystalline diffraction pattern is reestablished, when a previously shear aligned sample is sheared for a few seconds at shear rates below 5 s^{-1}). Each transition has a clear rheological signature in the form of a separate stress plateau in response to increasing rates. It is usually argued that such structural transformations happen in order to make the flow easier and easier at higher rates. This picture seems to apply here since the plateaus in stress imply that, at both transitions, the state stable at higher rate has a lower viscosity than the one for lower rates. It is also intuitively appealing since oriented dense planes sliding on top of one another parallel to the shear plane obviously correspond to an easier flow than a plastically deformed disoriented polcrystalline texture; one so rationalizes the high-shear oriented state. But the question of the intermediate state remains open in this picture: we see no intuitive explanation for an easy shear with {211} planes parallel to the shear plane.

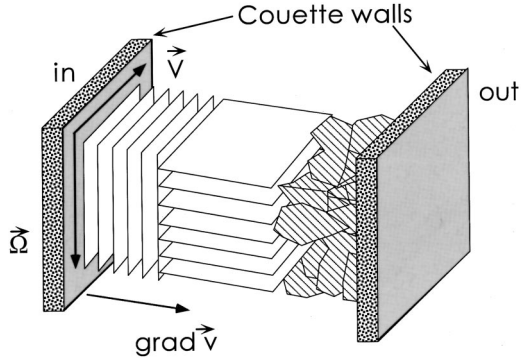

FIG. 7. Schematic representation of the three coexisting states of orientation at 50 s^{-1}. The parallel planes close to the inner wall and in the middle of the gap show the orientations of the dense {110} planes.

Plastic deformations of solid crystalline materials usually involve motion of dislocations over specific crystallographic planes (denoted {*abc*}) in definite crystallographic directions (denoted $\langle def \rangle$). This is called the slip mechanism. In bcc metals three principal slip systems have been observed: {110}⟨111⟩, {211}⟨111⟩, and {321}⟨111⟩. In each case, the slip direction corresponds to the most closely packed direction ⟨111⟩; as the energy of a dislocation is proportional to the square of the Burgers vector, dislocations of the shortest Burgers vector, that is, those along the close packed direction, will require the least stress. The most important slip

planes are also the most densely packed ({110} for bcc crystals), which are also the most widely separated. A higher shear stress is required to produce slip on planes of lower packing density. This is the reason why the {110}⟨111⟩ slip system is particularly active in bcc metals, whereas the two others are more marginal. Of course, comparing the two first slip systems in bcc metals with the two oriented steady states discussed here suggests that motion of dislocations may well play a crucial role in the flow behavior of our soft crystal. Following the above considerations on the energy of the dislocations, we would again expect gliding along the {110} planes to be preferred at any shear rate; the {211} orientation preferred at intermediate rates remains unexplained. Anyway, we should keep in mind that no basic principle supports the intuition that a texture allowing for an easier flow should necessarily take over; as a matter of fact, discontinuous shear thickening transitions have been reported in different contexts [18,22,23].

Returning now to rheological behavior and to the analogy mentioned in the Introduction, the stress plateaus in Fig. 1 are indeed reminiscent of the stress response of giant micelle solutions under shear at the orientation transition [13–15]. However, the analogy hides a basic difference. In the case of giant micelles, the initially uncorrelated orientations of individual micelles at rest couple to the flow when submitted to shear; the transition arises from the competition between the orienting effect of the shear and the disorienting effect of the thermal motion. After switching off the shear, the orientation becomes isotropic again. In that respect at least, speaking of a shear-induced ''phase transition'' makes some sense. The situation is different in the present study. The microscopic structure in all three different states of orientation is that of a bcc lattice with identical cell size. The orientation patterns then correspond to different macroscopic textures of the same phase and thermal motion plays no role: whatever the orientation induced during preshear, it survives identically after abrupt offset of the shear. Thinking in terms of a shear-induced ''phase transition'' is misleading.

[1] N. A. Clark and B. J. Ackerson, Phys. Rev. Lett. **44**, 1005 (1980).
[2] B. J. Ackerson and N. A. Clark, Phys. Rev. Lett. **46**, 123 (1981).
[3] B. J. Ackerson and N. A. Clark, Phys. Rev. A **30**, 906 (1984).
[4] Y. D. Yan, J. K. Dhont, C. Smits, and H. N. Lekkerkerker, Physica A **366**, 682 (1994).
[5] L. B. Chen, M. K. Chow, B. J. Ackerson, and C. F. Zukoski, Langmuir **10**, 2817 (1994), and references therein.
[6] P. Alexandridis, J. E. Holzwarth, and T. A. Hatton, Macromolecules **27**, 2414 (1994).
[7] K. Mortensen, Europhys. Lett. **19**, 599 (1992).
[8] G. A. McConnell and A. P. Gast, Macromolecules **30**, 435 (1997).
[9] J. A. Pople *et al.*, Macromolecules **30**, 5721 (1997); **31**, 2953 (1998).
[10] K. A. Koppl, M. Tirrell, F. S. Bates, K. Almaldal, and K. Mortensen, J. Rheol. **38**, 999 (1994).
[11] F. Molino, J.-F. Berret, G. Porte, O. Diat, and P. Lindner, Eur. Phys. J. B **3**, 59 (1998).
[12] G. A. McConnell, M. Y. Lin, and A. P. Gast, Macromolecules **28**, 6754 (1995).
[13] V. Schmitt, F. Lequeux, A. Pousse, and D. Roux, Langmuir **10**, 955 (1994).
[14] J.-F. Berret, D. C. Roux, and G. Porte, J. Phys. II **4**, 1261 (1994).
[15] R. Mahloufi, J. P. Decruppe, A. Ait-Ali, and R. Cressely, Europhys. Lett. **32**, 253 (1995).
[16] M. E. Cates, T. C. B. McLeish, and G. Marrucci, Europhys. Lett. **21**, 451 (1993).
[17] P. D. Olmsted and C.-Y. D. Lu, Phys. Rev. E **56**, 55 (1997).
[18] P. Sierro, Ph.D. thesis, Univeristy of Bordeaux, 1995 (unpublished).
[19] D. Bonn and J. Meunier, Phys. Rev. E **58**, 2115 (1998).
[20] However, while taking scattering data under steady shear at the highest rate (365 s^{-1}), we could observe in the patterns a slight deformation of the bcc lattice toward a distorted hcp structure (as reported in Ref. [3]). The distortion immediately vanishes after cessation of shear but the strong orientation remains. No distortion under shear could be detected at lower rates.
[21] I. W. Hamley, J. A. Pople, C. Booth, L. Derici, M. Imperor-Clerc, and P. Davidson, Phys. Rev. E **58**, 7620 (1998).
[22] A. M. Wunderlich and P. O. Bruun, Colloid Polym. Sci. **267**, 627 (1989).
[23] M. K. Chow and C. F. Zukoski, J. Rheol. **39**, 15 (1995).